## RESEARCH ARTICLE

# Haustral rhythmic motor patterns of the human large bowel revealed by ultrasound

Amer Hussain,[1] Zhenyu Zhang,[1,2] Jennifer Yu,[3] Ruihan Wei,[3] Hamza Arshad,[3] Jinhwan Lew,[3] Cierra Jagan,[3] Yongdong Wang,[4] Ji-Hong Chen,[1] and Jan D. Huizinga[1,2]

[1]Department of Medicine, McMaster University, Hamilton, Ontario, Canada; [2]Department of Biomedical Engineering, McMaster University, Hamilton, Ontario, Canada; [3]Biomedical Engineering, University of Waterloo, Waterloo, Ontario, Canada; and [4]Department of Radiology, McMaster University, Hamilton, Ontario, Canada

## Abstract

Effective and widely available strategies are needed to diagnose colonic motility dysfunction. We investigated whether ultrasonography could generate spatiotemporal maps combined with motor pattern frequency analysis, to become a noninvasive method to characterize human colon motor patterns. Abdominal colonic ultrasonography was performed on healthy subjects (N = 7), focusing on the detailed recording of spontaneous haustral activities. We developed image segmentation and frequency analysis software to analyze the motor patterns captured. Ultrasonography recordings of the ascending, transverse, and descending colon identified three distinct rhythmic motor patterns: the 1 cycle/min and the 3 cycles/min cyclic motor pattern were seen throughout the whole colon, whereas the 12 cycles/min cyclic motor pattern was identified in the ascending colon. The rhythmic motor patterns of the human colon that are associated with interstitial cells of Cajal-associated pacemaking activity can be accurately identified and quantified using ultrasound.

**NEW & NOTEWORTHY** Ultrasonography in the clinical field is an underutilized tool for assessing colonic motility; however, with the addition of frequency analysis techniques, it provides a method to identify human colonic motor patterns. Here we report on the 1, 3, and 12 cpm rhythmic motor patterns. Ultrasound has the potential to become a bedside assessment for colonic dysmotility and may reveal the health of interstitial cells of Cajal (ICC) pacemaker activities.

*colonic motility; cyclic motor patterns; interstitial cells of Cajal; ultrasonography*

## INTRODUCTION

Ultrasound is a noninvasive tool that can provide real-time visualization of the gastrointestinal tract (1). Motility can be observed in a natural state without sedatives, although full characterization of motor patterns will require the development of analysis techniques for spatiotemporal mapping. Most diagnoses of motility disorders are subjective, based on clinical signs such as stool morphology and defecation frequency rather than physiological measurements of motility (2). The most advanced technique for assessing colonic motility is high-resolution colonic manometry (HRCM) using catheters with 1 cm spaced sensors that cover the entire colon (3). Using the HRCM technique, major recent advances have been made in understanding physiology and diagnosing the pathophysiology of colonic dysmotility in patients (3–7). However, HRCM has disadvantages as it is costly, time-consuming, and invasive, and ultrasonography may become an alternative (8). Since ultrasonography, by its nature, will focus on a 4–5-cm length of the colon, it will capture motility within 2–4 haustra.

Dinning and coworkers have shown that the most common motor pattern of the human colon is a low-frequency "cyclic motor pattern," a pattern that shows pressure waves at 2–6 cycles/min over a length of ∼4–10 cm, commonly referred to as the 3 cpm cyclic motor pattern, since that frequency dominates. Furthermore, they showed that this motor pattern might not be evoked by a meal in patients with constipation, unlike healthy subjects, which was suggested to be due to neuropathy in the extrinsic parasympathetic innervation of the colon (9). Recently, we found the 3 cpm cyclic motor pattern to be absent in most patients with chronic constipation, which was associated with high sympathetic tone measured using heart rate variability techniques (4). The cyclic motor pattern can be confined to a single haustrum or a few haustra throughout the colon (7, 10), and it is also prominent in the rectum (10, 11). The absence of the 3 cpm motor pattern may become a biomarker for dysmotility in chronic constipation.

The present study characterizes spontaneous rhythmic motor patterns of the human colon, observed without sedation or invasive techniques, captured by ultrasonography. The developed analysis techniques characterize their occurrence, intrinsic frequency, and amplitude.

## MATERIALS AND METHODS

### Participants

Seven healthy participants, 20–27 yr, 4 female, were recruited for abdominal bowel ultrasonography. Participants did not have a prior history of cardiovascular or gastrointestinal disease and were not taking any medications that affected their cardiac or gastrointestinal function. The study was conducted at McMaster University with ethics approvals obtained from McMaster University, Hamilton Integrated Research Ethics Board (Approval No. 12580), with written consent from all participants.

### Ultrasonography

Ultrasonography was performed with the Z-ONE ultrasound system (MindRay). Volunteers prepared for ultrasonography by performing a bowel cleansing the night before, followed by drinking 1.5 L of sorbitol just before the ultrasound. Sorbitol will remove gas and suspend solids, and the water (that is poorly absorbed due to the sorbitol) gives good contrast. Ultrasonography was done by finding colon locations that were active and visually clear such that both the top and bottom luminal wall were visible, since that is a requirement for the method of analysis. The probe was held in a fixed position to record for 5–10 min in longitudinal orientation to capture motor patterns. Several recordings were taken of each section of the colon, including ascending, transverse, and descending colon, when found to be optimal for ultrasound recording for each subject. The sigmoid and rectum were not captured as they did not provide quality imaging for capturing motor patterns because of their depth. Areas of overlapping colonic regions were avoided. A summary of the sections included in this report is found in Supplemental Fig. S1 (see https://doi.org/10.6084/m9.figshare.22572688.v2).

### Software and Language

We developed the software to create a Bowel Sonography Analysis program to generate spatiotemporal maps and frequency analysis in Python with the following libraries: OpenCV, scikit-image (v. 0.19), scikit-learn, and PyWavelets (v. 1.20). All figures were made with Matplotlib.

### Development of Our Bowel Sonography Analysis Program

We first selected a region of interest (ROI) window manually at the beginning of a recording that includes the top and bottom haustra wall (for more information see https://doi.org/10.5281/zenodo.8135841). There is no requirement for the size of the ROI window, it but should not cover the black region outside of the actual recording window.

AQ: 8

Image segmentation was developed with the objective of capturing rhythmic motor patterns at distinct frequencies (range = 0.5–20 cpm). We leveraged existing methods from computer visions and signal processing libraries in Python to measure the diameter change within and across the haustra from a 5–10 min video recording. We tested established convolution neural network backbones and traditional histogram-based methods for image segmentation. We opted for the latter method, which produced similar results but was faster in practice. The selected ROI region was down-sampled and preprocessed with a bilateral filter to remove sparkling noise from the ultrasound recording. The processed image was then segmented using mean-shift clustering or Otsu thresholding depending on the contrast ratio of the recording. After the segmentation, an edge detection filter was applied to identify the rectal walls. We measured the wall locations in eight sections of the ROI. For example, in a $256 \times 256$ (Width $\times$ Height) ROI image, the image was cropped into eight $32 \times 256$ equally spaced patches, and therefore eight distance measures were made. The distance was measured independently in each section. We dealt with artifacts or shadows that may disrupt the measurement in each section separately. In other words, we took into account any artifacts that may show up during the process by dividing the image into different parts to remove artifacts. Each segment was spatially close, and if an artifact was present in one segment, it was detected and the program referred back to a previous image so as not to lose all the information from that image. A spatial consistency model (https://gaussianbp.github.io/) was used to interpret the occluded region and smooth out adjacent regions. If all regions failed to make consistent measures, pure Gaussian noise was sampled instead of reusing measurements from the previous frame. The distances were then measured by calculating the vertical pixel-level distance between the two haustrum walls. The pixel distance was converted into centimeters based on the scale provided within the sonography recording. The diameter changes were measured at 10 locations across the haustral walls to reduce variance and measurement errors sudden appearance of gas that will create distortion of the wall detection. The PyWavelets software was used for continuous wavelet transforms and data analysis.

"Optical flows" were used to track the "horizontal" movement of the haustrum due to breathing, and we corrected for this movement. The program measures the optical flow using the OpenCV built-in Lucas-Kanade method to adjust the ROI accounting for horizontal movement per frame.

To calculate motor pattern frequency, the sampled time-series data were analyzed with the continuous wavelet transform to observe changes in frequency over time and better visualization of frequency components. To calculate the global frequency, we applied singular value decomposition on the data matrix and computed the Fourier transform on the first principal vector. We used the power spectrum density from the fast Fourier transforms as a comparison, albeit the lower frequency was distorted due to the nonstationarity in the original signal. It is worth noting that the frequency interpolated by Fourier analysis does not necessarily translate to cpm but instead is based on the duration of repetitive contraction during sonography (similar to wave functions). However, it was found to match with observations and was used to infer the underlying patterns. The diameters of the haustral regions were measured at the rate of 10–12 Hz, depending on the ultrasound settings. During image segmentation, the boundaries between two adjacent haustra were generally not included in the assessment of luminal diameter change. We created the program such that four different

**A**

**B**
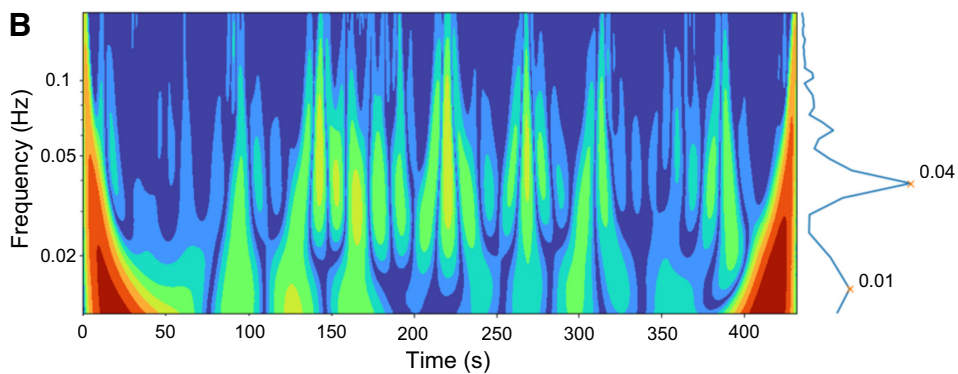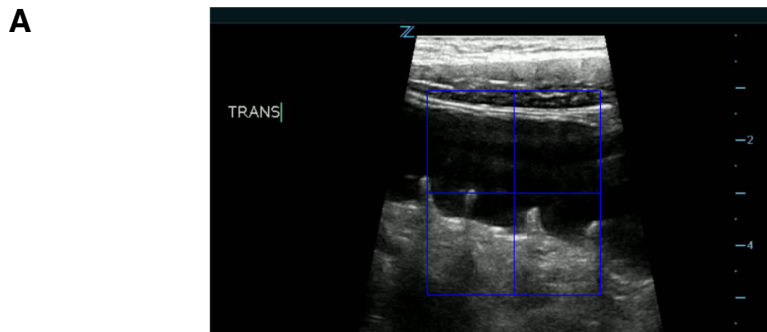


**Figure 1.** Sample of ultrasonography image and frequency analysis. *A*: sonography still image where the blue box is an ROI to be tracked for diameter change. The program identifies the borders of the haustrum and tracks their distance over time. The ruler is found on the right side of the recording in centimeters. *B*: wavelet plot from sonography recording identifying frequencies over time, showing dominant cyclic activity at 2.4 cpm (0.04 Hz) and 0.6 cpm (0.01 Hz). ROI, region of interest.

maps were generated: *1*) diameter maps, *2*) spatiotemporal maps, *3*) wavelet plots, and *4*) breathing displacement maps.

### Diameter Mapping

Diameter mapping illustrates the luminal diameter change of a selected region or region of interest (ROI, Fig. 1), which includes 1–3 haustra of the colon, over time, that is manually selected within a sonography video (Fig. 2A). The diameter mapping quantitatively shows the luminal diameter change that occurs over time, represented as a line graph, thus showing when contractions occur. An increase in diameter represents relaxation as the distance between the luminal walls increases, whereas a decrease represents contraction, hence the reverse y-axis scale.

### Spatiotemporal Mapping

The spatiotemporal mapping represents the contractions and relaxations across 1–3 haustra over time, where the oral-facing side of the lumen (denoted with a blue "Z" in sonography) associates with the top of the spatiotemporal mapping, whereas the anal-facing side of the lumen is associated with the bottom of the spatiotemporal mapping (Fig. 2A). In the spatiotemporal map, darker shades of blue and black are associated with increased lumen diameter or the relaxation of circular muscle. In contrast, green to red is associated with circular muscle contraction.

### Wavelet Plot

The wavelet plot illustrates the power (postlogarithmic transformation) of the frequencies recorded during so-nography, as in Fig. 1B, where frequency (in Hz) is on the y-axis and time (seconds) is on the x-axis. The average di-ameter change was obtained using sample medians at each sampling time. The power is represented by a color scale similar to spatiotemporal mapping. Figure 1B shows a wavelet example with the most significant frequencies (most power) observed at 0.04 and 0.01 Hz, or 2.4 and 0.6 cpm, respectively. The strength of the frequency is calcu-lated by FFT using Welch's method with a window size of 200 s to minimize spectral leakages.

## RESULTS

Ultrasonography was performed on healthy volunteers, where recordings were taken of several sections of the ascend-ing, transverse, and descending colon (capture 2–4 haustra) to capture motor patterns, as the colon can be quiet at times. Video recordings of 5–10 min were analyzed by creating spa-tiotemporal maps and subsequent frequency analyses devel-oped for the present study (see MATERIALS AND METHODS).
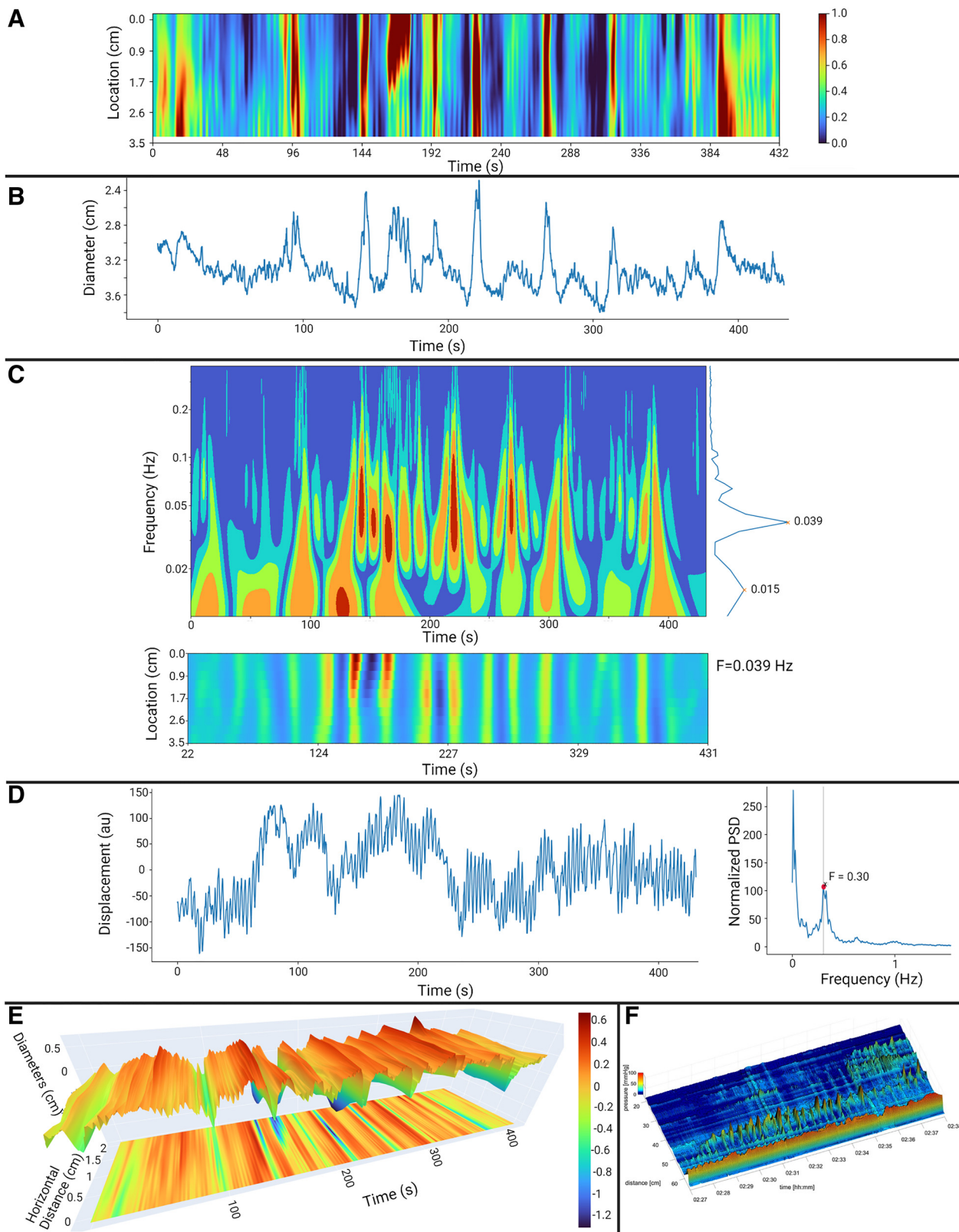
### The 3 Cpm Cyclic Motor Pattern

The 3 cpm cyclic motor pattern was the dominant motor activity observed. The average frequency was $2.6 \pm 0.6$ cpm, ranging from 1.8 to 3.7 cpm, and captured in the ascending, transverse, and descending colon ($N = 7$; $n = 10$). An individual contraction within a burst of 3 cpm ac-tivity showed a contraction that took ~5–10 s to fully con-tract before relaxing slowly over the following 15–25 s, with a propagation velocity of ~1 cm/s. Figure 2A shows a typical spatiotemporal map based on a video recording capturing 2 haustra at the ascending colon. The dominant contraction pattern occurred at 2.3 cycles/min as deter-mined by wavelet frequency analysis (Fig. 2C). Breathing occurred at 18 breaths/min as determined by the displace-ment map that monitors horizontal movements due to breathing (Fig. 2D). The spatiotemporal map (Fig. 2A) also

shows this breathing frequency; hence, the colon diameter changes due to breathing, which is superimposed on the colonic contraction pattern (Fig. 2B). Contractions are sometimes confined to a single haustrum (see Fig. 2A), but most contractions are synchronized across the haustra. A propagation velocity is usually difficult to determine since most contractions within the cyclic motor pattern appear simultaneous across the haustra, consistent with the findings using high-resolution colonic manometry (Fig. 2F; 12).

F3 Figure 3 shows ultrasonography data from an 8 min recording (Supplemental Video: https://doi.org/10.6084/m9.figshare.22572688.v2) from a segment of the descending colon that was 4.1 cm in length. As illustrated in a diameter map (Fig. 3B), the colon showed continuous rhythmic contraction-relaxation activity with an average contraction frequency of ~3 cpm. The motor pattern showed mixed antegrade and retrograde propagation, associated with turbulent flow. The wavelet plot (Fig. 3C) shows the dominant frequency at 2.4 cpm, with peaks also seen at 3.1 and 3.7 cpm; hence, the frequency range was 2.4–3.7 cpm, thus representing the typical 3 cpm cyclic motor pattern. Using frequency analysis, we can isolate the motor pattern at the dominant frequency of 2.4 cpm (Fig. 3C). Figure 3D shows the frequency of the horizontal breathing adjustment to the ROI at 0.28 Hz or 16.8 breaths/min.

### The 1 Cpm Rhythmic Motor Pattern

The 1 cpm rhythmic motor pattern was seen throughout the colon.

F4 Figure 4A shows still images of an ultrasonography recording that captures movements of 2–3 haustra, a bowel length of 4.2 cm, and horizontal displacements due to breathing. Figure 4B shows the spatiotemporal map from which horizontal breathing movements shown in Fig. 4E were removed. The 6-min map shows strong circular muscle contractions (Fig. 4, B and C) of irregular duration and frequency and an average frequency of 0.9 cpm. Three areas of deep relaxation (shown in black in Fig. 4B) were observed to be ~25–35 s in duration, during which dominant antegrade flow occurred in combination with the retrograde and turbulent flow (Fig. 4C). The wavelet plots (Fig. 4D) show the most dominant frequency to be 0.015 Hz or 0.9 cpm. The breathing rate during this recording can be inferred from the horizontal adjustments to the ROI for the breathing interference (Fig. 4E), which was 0.24 Hz (~14 breaths/min).

F5 Figure 5 shows a dominant frequency of 1.2 cpm with the 3.2 cpm cyclic motor pattern superimposed. The average frequency of this motor pattern was $1.14 \pm 0.2$ cpm, ranging from = 0.9 to 1.4 cpm, and captured in the ascending and descending colon ($N = 5$; $n = 6$).

### The 12 Cpm Cyclic Motor Pattern

The 12 cpm cyclic motor pattern reported previously using F6 HRCM was observed in the descending colon (Fig. 6, A and C) (7). Figure 6, A and B, shows bursts of cyclic activity. The wavelet frequency analysis (Fig. 6C) captures 1 cpm bursts of rhythmic motor activity, dominated by a 12-cpm cyclic motor pattern, clearly distinguished from the consistent and continuous breathing frequency of 16.4 cpm, as seen in Fig. 6D. The bursts represent a high-amplitude pressure wave (HAPW) since HAPWs are composed of 12 cpm pressure waves (10).

## DISCUSSION
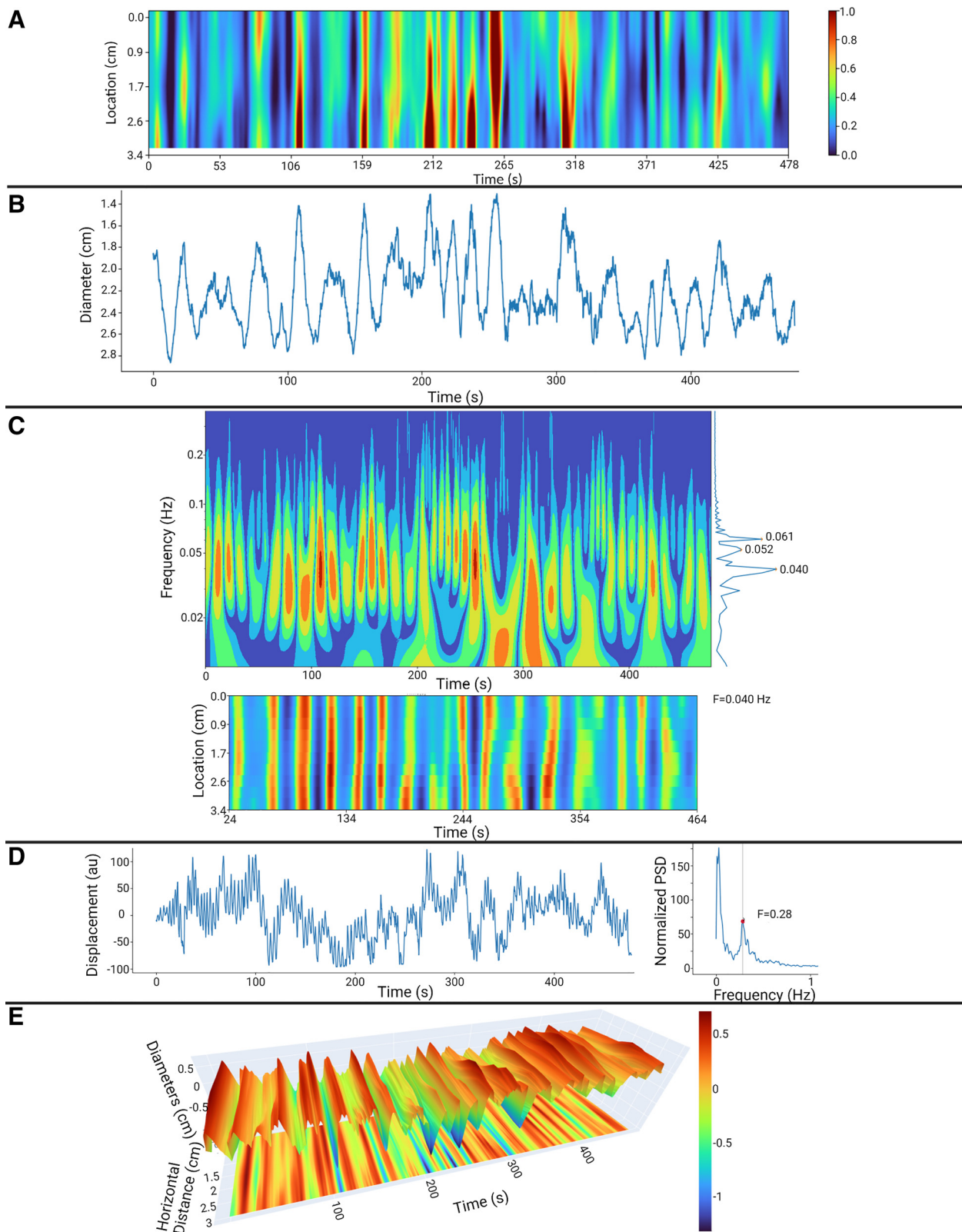
The 3 cpm cyclic motor pattern is one of the human colon's dominant motor activities and was the present study's dominant motor pattern, seen in the cecum-ascending colon, the transverse colon, and the descending colon. This motor pattern was demonstrated previously using electrical recordings and pressure measurements (10, 13–15), and here we show that ultrasound cannot only faithfully capture this motor pattern but also its association with content flow. The turbulent nature of the associated flow suggests that its main function is content mixing for absorption and stool formation. Colon motility is designed to prevent continuous transit into the rectum that would give rise to a continuous urge to defecate (10, 16). The rectosigmoid brake hypothesis was reported on by Lin et al. (6), which points to the prominence of retrograde propagation of this motor pattern in the sigmoid and rectum (6, 10).

The 12 cpm cyclic motor pattern was first described by us as a distinct cyclic motor pattern using HRCM (10). It was also seen in electrical recordings of the human colon in vivo (13). The 12 cpm activity is proposed to underlie the HAPWs such that the HAPW is a result of transient activation of the 12-cpm interstitial cells of Cajal (ICC) pacemaker activity that results in contractions at this frequency unless the amplitude is high, which then results in contraction summation, forming the HAPW. Since the HAPW is generated infrequently, it is expected to be seen by ultrasound infrequently, and it will require a stimulus such as rectal stimulation to be observed during a relatively short ultrasound assessment.

The 1 cpm cyclic motor pattern was captured in both the ascending and descending colon. The patterns consisted of an irregular duration of the contraction phase followed by 25–35 s of relaxation, which involved antegrade, retrograde, and turbulent flow, with a slightly greater prevalence of turbulent and antegrade flow as seen from ultrasonography (Supplemental Material: https://doi.org/10.6084/m9.figshare.22572688.v2). The 1 cpm motor pattern appears to be important for transit and absorption; previous studies have demonstrated low-frequency, high-amplitude contractions that occur between 0 and 1 cpm in the human colon (17–19). This motor pattern appears to persist in colonic in vitro strips devoid of the interstitial cells of Cajal of the submuscular plexus (ICC-SMP) network associated with the submuscular plexus (17). Since it is shown to be tetrodotoxin resistant, it is hypothesized that the 1 cpm rhythmic motor pattern is of myogenic origin and associated with ICC of the myenteric plexus (ICC-MP) evoked by excitatory neural inputs related to stretch or distention of the colon (20).

In concert with the autonomic nervous system, four networks of ICC orchestrate haustral motor patterns throughout

---

**Figure 2.** Ultrasonography of the ascending colon involving 3 haustra. All images are from one male subject. A: spatiotemporal map with subtraction of horizontal movement artifact due to breathing (Supplemental Video E12_C2: https://doi.org/10.6084/m9.figshare.22572688.v2). B: diameter map tracking average diameter change in the ROI (segment of the colon) over time. C: wavelet plot to analyze frequency components over time along with contraction plot over time with the most power at 0.039 Hz or 2.3 cpm. D: breathing displacement map, the horizontal displacements of the ROI box, with 0 as the original placement. The frequency plot shows frequencies with the most significant powers corresponding to the horizontal displacement due to breathing. E: three-dimensional (3-D) spatiotemporal map of contractions that occur down the length of the segment of the colon over time after subtraction of horizontal movement artifact due to breathing. F: spatiotemporal map obtained through high-resolution colonic manometry showing a cyclic motor pattern as pressure waves (10). ROI, region of interest.

**Figure 3.** Ultrasonography of the descending colon involving 3 haustra. All images from one male subject. *A*: spatiotemporal map (Supplemental Video E12_C5: https://doi.org/10.6084/m9.figshare.22572688.v2). *B*: diameter map. *C*: wavelet plot along with contraction plot with the most power at 0.04 and 0.06 Hz or 2.4 and 3.6 cpm, respectively. *D*: breathing displacement map. *E*: three-dimensional (3-D) spatiotemporal map.

**Figure 4.** Ultrasonography of the descending colon involving 2–3 haustra. All images from one female subject. *A*: static image from ultrasonography recording (Supplemental Video E1_C37: https://doi.org/10.6084/m9.figshare.22572688.v2). *B*: spatiotemporal map. *C*: diameter map. *D*: wavelet plot along with contraction plot with the most power at 0.015 and 0.044 Hz or 0.9 and 2.6 cpm, respectively. *E*: breathing displacement map. *F*: three-dimensional (3-D) spatiotemporal map.

AQ: 17
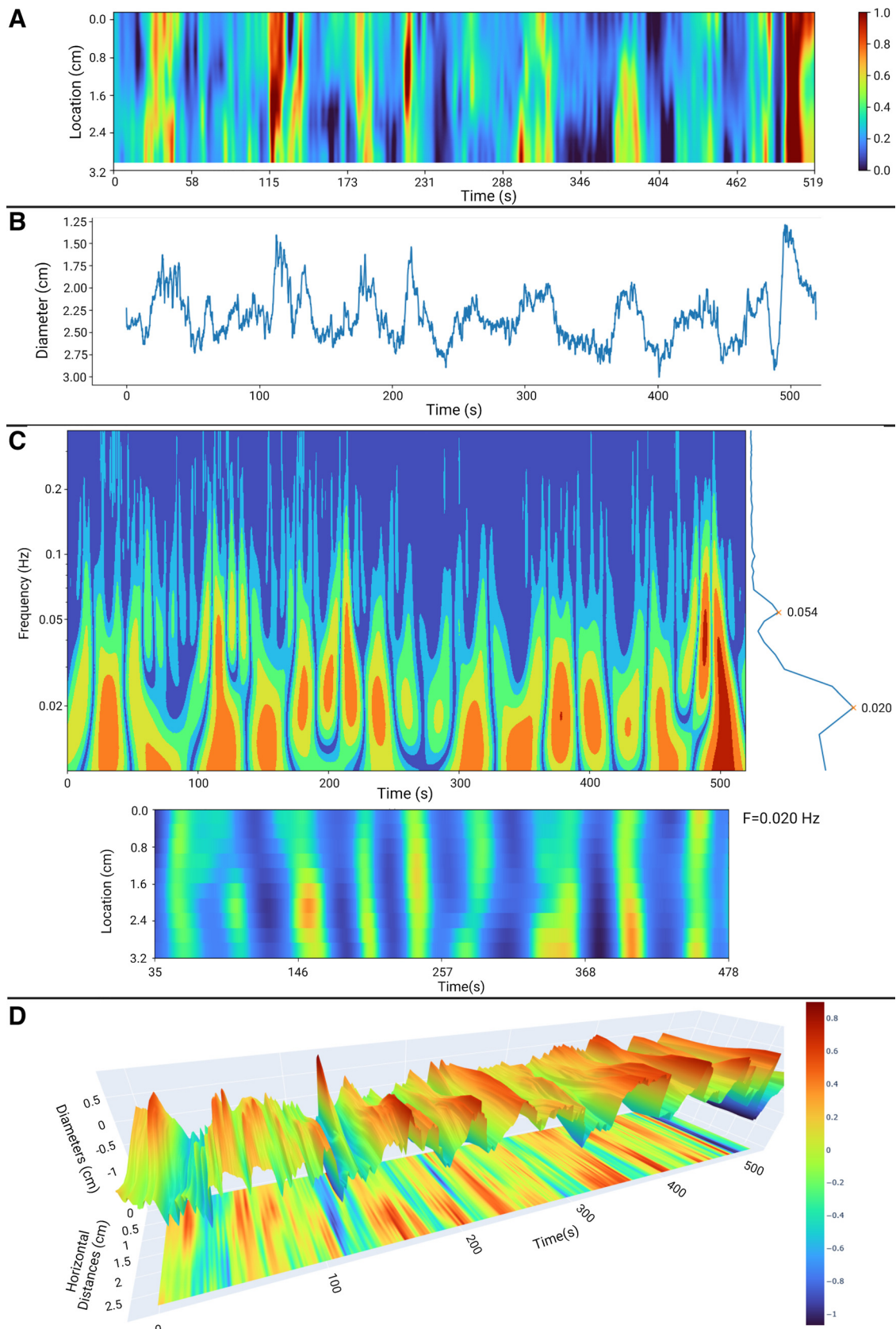
**Figure 5.** Ultrasonography of the descending colon involving 2–3 haustra. All images from one female subject. *A*: spatiotemporal map (Supplemental Video E13_C6: https://doi.org/10.6084/m9.figshare.22572688.v2). *B*: diameter map. *C*: wavelet plot along with contraction plot with the most power at 0.020 and 0.054 Hz or 1.2 and 3.24 cpm, respectively. *D*: three-dimensional (3-D) spatiotemporal map.
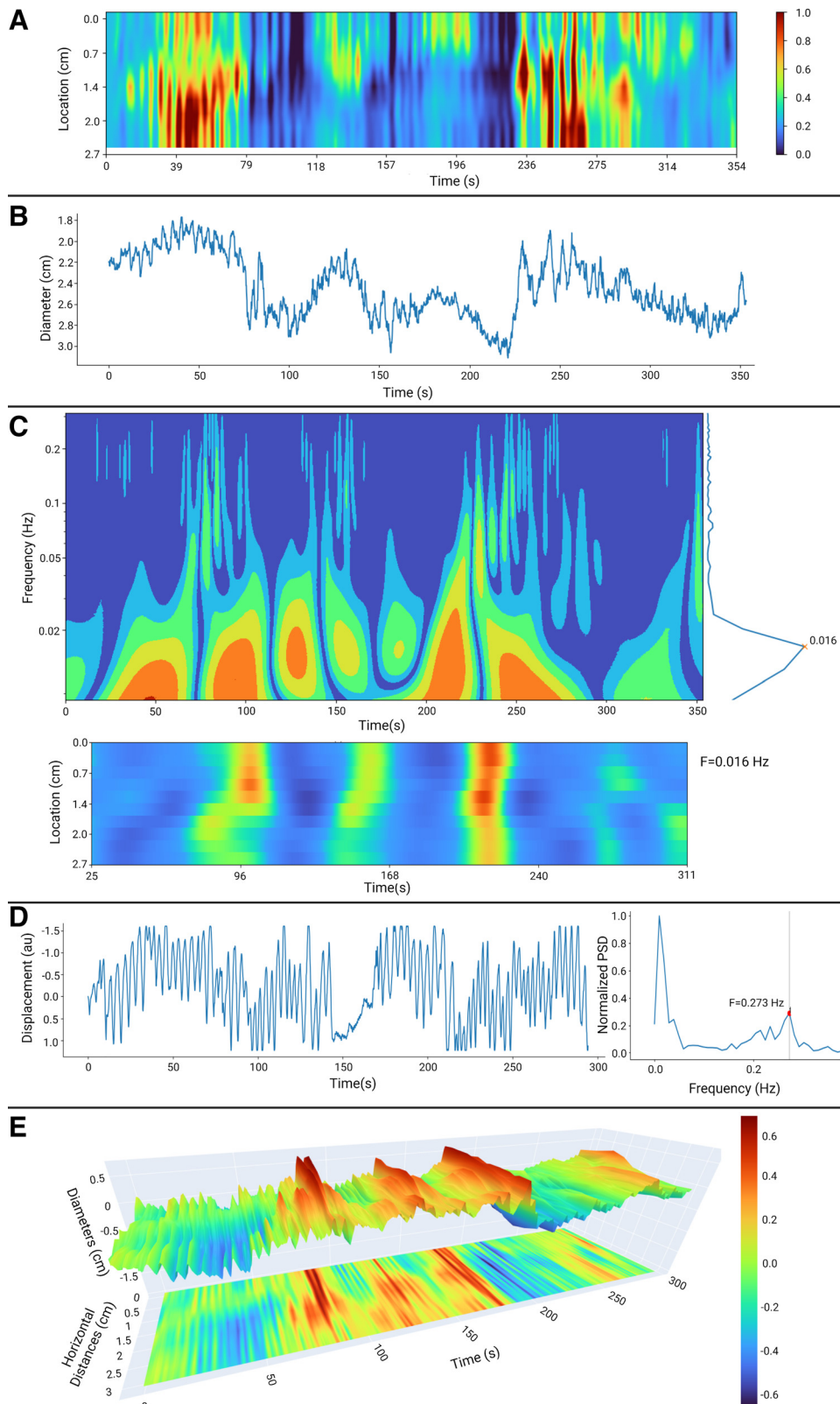
**COLOR**

**Figure 6.** Ultrasonography of the ascending colon involving 2–3 haustra. All images from one male subject. *A*: spatiotemporal map (link Supplemental Video E3_C1: https://doi.org/10.6084/m9.figshare.22572688.v2). *B*: diameter map. *C*: wavelet and contraction plots with the most power at 0.016 Hz or 0.96 cpm. In addition, a frequency of 12 cpm can also be seen in spatiotemporal and diameter maps, where the wavelet shows a high frequency pattern that differs from the breathing frequency (*D*, 16.38 cpm). *D*: breathing displacement map. *E*: three-dimensional (3-D) map of *A*.

the human colon. ICC associated with the myenteric plexus or ICC-MP function as stimulus-dependent pacemaker cells that orchestrate high-amplitude pressure waves and the associated 12 cpm high-frequency cyclic motor pattern (16).

A second ICC network is associated with the submuscular plexus, the ICC-SMP, which functions as the dominant pacemaker cells of the human colon, generating the 3 cpm cyclic motor pattern (10, 21). A third network is the intramuscular

ICC (interstitial cells of Cajal of the intermuscular plexus, ICC-IM), present in both the longitudinal and circular muscles. The ICC-IM is involved in transmitting pacemaker activity throughout the musculature and mediating neural stimuli from the autonomic nervous systems (10, 22). Finally, a fourth ICC network is associated with the subserosa, or interstitial cells of Cajal of the subserosa plexus (ICC-SS; 23), which may play a role in the pacemaker functions of the longitudinal muscle layer within the colon (24, 25).

An important part of generating informative spatiotemporal maps was the removal of movement due to breathing, the horizontal movement of the entire colon in view. Even after removal, contractions and relaxations at the breathing frequency are still visible. In addition, from sonography recordings, content can be seen to be mixing due to antegrade and retrograde movements, resulting in turbulent flow in relation to breathing. It may be hypothesized that the act of breathing provides mechanical stimulation to the colon. By inhaling and exhaling, expansion and contraction of the diaphragm provide mechanical stimulation. In addition, breathing also influences the autonomic nervous system at the breathing frequency, a phenomenon called respiratory sinus arrhythmia (RSA), potentially providing stimulation and inhibition to the colon at the breathing frequency.

Our goal is to develop ultrasonography for determining dysmotility. A limitation of the technique is that it is challenging to capture motor patterns that may only arise once every few hours, such as the HAPW (or HAPC, high amplitude propagating contraction). This may be overcome by assessing motor patterns in response to a stimulus. We found that rectal stimulation with bisacodyl is a reliable stimulus to evoke HAPWs (4, 5). A meal is not optimal with ultrasonography, as 1.5 L of sorbitol is taken before ultrasound, and a subsequent meal intake would provide discomfort. In addition, motor patterns evoked by a meal may not appear immediately or consistently.

**AQ: 9**

**AQ: 10**

One issue is the low signal-to-noise ratio when the contractions are weak. The currently implemented solution is to combine independent samples with random perturbation of local subsamples. Improving the signal-to-noise ratio using more advanced segmentation algorithms such as U-Net will relax this assumption. Our current approach for propagation velocity measurements is to calculate the instantaneous phase synchrony between each sample location through a complex wavelet transform. However, the result tends to have high variance and requires human fine-tuning. Furthermore, visual-based flow tracking with ultrasound proved difficult due to the natural limitations of the two-dimensional (2-D) field of view. The presence of small fecal content is relied upon to measure flow, but such particles often disappear in subsequent frames, which makes traditional sparse optical flow tracking (Lucas-Kanade) not feasible.

One of the challenges is the measurement of false wall boundaries due to the colonic wall "disappearing," out of focus, during contractions. In addition, the visual contrast between the wall, content (such as fecal matter), and gas in the ultrasound images can be limited as the ultrasound provides black-and-white recording, which complicates the task of distinguishing between different structures for the

purpose of image segmentation. Ideally, a program should allow for the manual correction of such artifacts.

In summary, within the human colon, rhythmic motor patterns result from the communication between musculature, efferent enteric and extrinsic autonomic nerves, and several networks of ICC. ICC determines many of the properties of colonic motor patterns, such as the frequency, velocity, and direction of propagation, which can be visually measured via ultrasonography. We show here that filtering breathing frequency followed by frequency analysis allows for characterizing individual motor patterns that occur within and across haustra. Further development of the techniques to characterize not only spontaneous motor patterns but also those that occur following a stimulus, such as rectal stimulation, will result in a noninvasive methodology for determining motility dysfunction.

## DATA AVAILABILITY

Data will be made available upon reasonable request.          **AQ: 11**

## SUPPLEMENTAL DATA

Supplemental videos and figure: https://doi.org/10.6084/m9. **AQ: 12**
figshare.22572688.v2.

The segmentation program at its current state: https://doi.org/ 10.5281/zenodo.8135841.          **AQ: 13**

## ACKNOWLEDGMENTS

Figures and graphical abstract were created with Biorender. com.

## GRANTS

## DISCLOSURES

No conflicts of interest, financial or otherwise, are declared by the authors.          **AQ: 15**

## AUTHOR CONTRIBUTIONS

A.H., J.-H.C., and J.D.H. conceived and designed research; A.H. and Y.W. performed experiments; A.H. and Z.Z. analyzed data; A.H. and Z.Z. interpreted results of experiments; A.H. and Z.Z. prepared figures; A.H. drafted manuscript; A.H., Z.Z., J.Y., R.W., H.A., J.L., C.J., Y.W., J.-H.C., and J.D.H. edited and revised manuscript; A.H., J.Y., R.W., H.A., J.L., C.J., Y.W., J.-H.C., and J.D.H. approved final version of manuscript.          **AQ: 16**

## REFERENCES

1. **Maconi G, Radice E, Bareggi E, Porro GB.** Hydrosonography of the gastrointestinal tract. *Am J Roentgenol* 193: 700–708, 2009. doi:10.2214/AJR.08.1979.

2. **Fox MR, Kahrilas PJ, Roman S, Gyawali CP, Scott SM, Rao SS, Keller J, Camilleri M; International Working Group for Disorders of Gastrointestinal Motility and Function.** Clinical measurement of gastrointestinal motility and function: who, when and which test?

*Nat Rev Gastroenterol Hepatol* 15: 568–579, 2018. doi:10.1038/s41575-018-0030-9.

3. **Li YW**, **Yu YJ**, **Fei F**, **Zheng MY**, **Zhang SW.** High-resolution colonic manometry and its clinical application in patients with colonic dysmotility: a review. *World J Clin Cases* 7: 2675–2686, 2019. doi:10.12998/wjcc.v7.i18.2675.

4. **Liu L**, **Milkova N**, **Nirmalathasan S**, **Ali MK**, **Sharma K**, **Huizinga JD**, **Chen JH.** Diagnosis of colonic dysmotility associated with autonomic dysfunction in patients with chronic refractory constipation. *Sci Rep* 12: 12051, 2022. doi:10.1038/s41598-022-15945-6.

5. **Milkova N**, **Parsons SP**, **Ratcliffe E**, **Huizinga JD**, **Chen J-H.** On the nature of high-amplitude propagating pressure waves in the human colon. *Am J Physiol Gastrointest Liver Physiol* 318: G646–G660, 2020. doi:10.1152/ajpgi.00386.2019.

6. **Lin AY**, **Du P**, **Dinning PG**, **Arkwright JW**, **Kamp JP**, **Cheng LK**, **Bissett IP**, **O'grady G.** High-resolution anatomic correlation of cyclic motor patterns in the human colon: evidence of a rectosigmoid brake. *Am J Physiol Gastrointest Liver Physiol* 312: G508–G515, 2017. doi:10.1152/ajpgi.00021.2017.

7. **Huizinga JD**, **Pervez M**, **Nirmalathasan S**, **Chen JH.** Characterization of haustral activity in the human colon. *Am J Physiol Gastrointest Liver Physiol* 320: G1067–G1080, 2021. doi:10.1152/AJPGI.00063.2021.

8. **Kishi K**, **Kaji N**, **Tsuru Y**, **Hori M.** A novel noninvasive method for quantitative detection of colonic dysmotility using real-time ultrasonography. *Digestion* 102: 731–741, 2021. doi:10.1159/000511851.

9. **Dinning PG**, **Wiklendt L**, **Maslen L**, **Patton V**, **Lewis H**, **Arkwright JW**, **Wattchow DA**, **Lubowski DZ**, **Costa M**, **Bampton PA.** Colonic motor abnormalities in slow transit constipation defined by high-resolution, fibre-optic manometry. *Neurogastroenterol Motil* 27: 379–388, 2015. doi:10.1111/nmo.12502.

10. **Pervez M**, **Ratcliffe E**, **Parsons SP**, **Chen JH**, **Huizinga JD.** The cyclic motor patterns in the human colon. *Neurogastroenterol Motil* 32: e13807, 2020. doi:10.1111/nmo.13807.

11. **Rao SSC**, **Sadeghi P**, **Beaty J**, **Kavlock R**, **Ackerson K.** Ambulatory 24-h colonic manometry in healthy humans. doi:10.1152/ajpgi.2001.280.4.G629.

12. **Chen JH**, **Parsons SP**, **Shokrollahi M**, **Wan A**, **Vincent AD**, **Yuan Y**, **Pervez M**, **Chen WL**, **Xue M**, **Zhang KK**, **Eshtiaghi A**, **Armstrong D**, **Bercik P**, **Moayyedi P**, **Greenwald E**, **Ratcliffe EM**, **Huizinga JD.** Characterization of simultaneous pressure waves as biomarkers for colonic motility assessed by high-resolution colonic manometry. *Front Physiol* 9: 1248, 2018. doi:10.3389/fphys.2018.01248.

13. **Bueno L**, **Fioramonti J**, **Frexinos J**, **Ruckebusch Y.** Colonic myoelectrical activity in diarrhea and constipation. *Hepatogastroenterology* 27: 381–389, 1980.

14. **Latimer P**, **Sarna S**, **Campbell D**, **Latimer M**, **Waterfall W**, **Daniel EE.** Colonic motor and myoelectrical activity: a comparative study of normal subjects, psychoneurotic patients, and patients with irritable bowel syndrome. *Gastroenterology* 80: 893–901, 1981. doi:10.1016/0016-5085(81)90056-1.

15. **Sarna SK**, **Bardakjian BL**, **Waterfall WE**, **Lind JF.** Human colonic electrical control activity (ECA). *Gastroenterology* 78: 1526–1536, 1980. doi:10.1016/s0016-5085(19)30512-8.

16. **Huizinga JD**, **Hussain A**, **Chen JH.** Interstitial cells of Cajal and human colon motility in health and disease. *Am J Physiol Gastrointest Liver Physiol* 321: G552–G575, 2021. doi:10.1152/ajpgi.00264.2021.

17. **Corsetti M**, **Costa M**, **Bassotti G**, **Bharucha AE**, **Borrelli O**, **Dinning P**, **di Lorenzo C**, **Huizinga JD**, **Jimenez M**, **Rao S**, **Spiller R**, **Spencer NJ**, **Lentle R**, **Pannemans J**, **Thys A**, **Benninga M**, **Tack J.** First translational consensus on terminology and definitions of colonic motility in animals and humans studied by manometric and other techniques. *Nat Rev Gastroenterol Hepatol* 16: 559–579, 2019. doi:10.1038/s41575-019-0167-1.

18. **Mañé N**, **Martínez-Cutillas M**, **Gallego D**, **Jimenez M.** Enteric motor pattern generators involve both myogenic and neurogenic mechanisms in the human colon. *Front Physiol* 6: 205, 2015. doi:10.3389/fphys.2015.00205.

19. **Rae MG**, **Fleming N**, **McGregor DB**, **Sanders KM**, **Keef KD.** Control of motility patterns in the human colonic circular muscle layer by pacemaker activity. *J Physiol* 510: 309–320, 1998. doi:10.1111/j.1469-7793.1998.309bz.x.

20. **Rosli RM**, **Heitmann PT**, **Kumar R**, **Hibberd TJ**, **Costa M**, **Wiklendt L**, **Wattchow DA**, **Arkwright J**, **de Fontgalland D**, **Brookes SJH**, **Spencer NJ**, **Dinning PG.** Distinct patterns of myogenic motor activity identified in isolated human distal colon with high-resolution manometry. *Neurogastroenterol Motil* 32: e13871, 2020. doi:10.1111/nmo.13871.

21. **Dinning PG**, **Wiklendt L**, **Maslen L**, **Gibbins I**, **Patton V**, **Arkwright JW**, **Lubowski DZ**, **O'Grady G**, **Bampton PA**, **Brookes SJ**, **Costa M.** Quantification of in vivo colonic motor patterns in healthy humans before and after a meal revealed by high-resolution fiber-optic manometry. *Neurogastroenterol Motil* 26: 1443–1457, 2014. doi:10.1111/nmo.12408.

22. **Ward SM**, **Beckett EAH**, **Wang X**, **Baker F**, **Khoyi M**, **Sanders KM.** Interstitial cells of Cajal mediate cholinergic neurotransmission from enteric motor neurons. *J Neurosci* 20: 1393–1403, 2000. doi:10.1523/JNEUROSCI.20-04-01393.2000.

23. **Rumessen JJ**, **Vanderwinden JM**, **Hansen A**, **Horn T.** Ultrastructure of interstitial cells in subserosa of human colon. *Cells Tissues Organs* 197: 322–332, 2013. doi:10.1159/000346314.

24. **Drumm BT**, **Rembetski BE**, **Messersmith K**, **Manierka MS**, **Baker SA**, **Sanders KM.** Pacemaker function and neural responsiveness of subserosal interstitial cells of Cajal in the mouse colon. *J Physiol* 598: 651–681, 2020. doi:10.1113/JP279102.

25. **Aranishi H**, **Kunisawa Y**, **Komuro T.** Characterization of interstitial cells of Cajal in the subserosal layer of the guinea-pig colon. *Cell Tissue Res* 335: 323–329, 2009. doi:10.1007/s00441-008-0730-5.

# AUTHOR QUERIES

## AUTHOR PLEASE ANSWER ALL QUERIES                                    1

AQau— Please confirm the given-names and surnames are identified properly by the colors. Names will appear in PubMed exactly as shown on the approved proofs.
   ■= Given-Name, ■= Surname

AQaff— Please confirm the Institutions and country names are identified properly by the colors given within the affiliation section.
   ■= Institution, ■= Country name

AQ1:— Please read entire proof (including query page), answer queries and mark corrections (using Adobe tools per online instruction), and return it within 2 business days to the online proof review site (link provided in email). IMPORTANT: Make sure query page is included. Please only make changes that are essential to correct data errors. Requests for cosmetic and other nonessential changes to figures and text at this stage will not be accommodated.

AQ2:— Please check all figures, tables, equations, and legends carefully. Changes will be made only to correct scientifically relevant errors. Please confirm or correct abbreviation definitions that have been inserted in the legends by the copy editor. If changes are required to the figures themselves, please list ALL changes requested (even if you provide a new figure).

AQ3:— Please note that your manuscript has been copyedited and that style changes have been made, including those related to punctuation, abbreviations, italics, hyphens and word divisions, units of measurement, etc., to conform to Journal style preferences. Please check that no errors in meaning were inadvertently introduced. Not all of the changes are pointed out in the Author Query list, so please check all text carefully.

AQ4:— Please carefully review the hierarchy of headings throughout your article.

AQ5:— Please confirm the edited affiliations are correct.

AQ6:— Please verify accuracy of your e-mail for correspondence. (Note: this material is listed as a footnote at bottom of left column of text on the first page .)

AQ7:— Please check any ORCID links in your manuscripts to ensure they link to the intended materials.

AQ8:— Please confirm that placement of the Zenodo link is correct.

AQ9:— Was "2-D" written out correctly as "two-dimensional"?

AQ10:— Please check the edits in the sentence "One of the challenges..." and revise/reject as needed.

AQ11:— APS now requires authors to explain their data sharing plan. Do the authors agree that "Data will be made available upon reasonable request" or should another statement be inserted in this section?

AQ12:— Please confirm the edited Supplemental Material information and links are correct.

# AUTHOR QUERIES

## AUTHOR PLEASE ANSWER ALL QUERIES                                    2

AQ13:— Please verify that all supplemental DOI links are public and active and access all intended
supplemental material.

AQ14:— Please confirm the edited Grants section is correct.

AQ15:— The text in the DISCLOSURES section reflects your data entry into the Peer Review sub-
mission. Is this still complete, relevant, and accurate?

AQ16:— The text in the AUTHOR CONTRIBUTIONS section reflects your data entry into the Peer
Review submission. Is this still complete and accurate? If changes are needed, please follow
this template.

AQ17:— Was "3-D" written out correctly as "Three-dimensional"?